Effects of anodizing conditions on anodic alumina structure

Nai-Qin Zhao · Xiao-Xue Jiang · Chun-Sheng Shi ·
Jia-Jun Li · Zhi-Guo Zhao · Xi-Wen Du

Abstract In this paper, two-step anodization was used to obtain porous anodic alumina (PAA) films, which are widely used as the temples to fabricate nanomaterials. Effects of anodizing conditions such as anodizing voltage and the concentration of electrolyte on steady current density (I_s) and anodic alumina structure were investigated for oxalic acid as an electrolyte. The result shows that I_s is dependent on anodizing voltage exponentially. The relationship between the concentration of electrolyte and the pore diameter is almost linear, while there is no effect on inner-pore distance. At different anodizing voltage, the effect degree of the concentration of oxalic acid on the pore diameter is various. In oxalic acid electrolyte with given concentration matching with a specifically anodizing voltage, optimal nano-pores arrangements can be obtained. The higher voltage induces the collapse of thin inner wall and disordered alumina nanowires (ANWs) were formed.

Introduction

Porous anodic alumina (PAA) growth on high purity aluminum by anodization in various acid electrolytes has been studied since 1953 [1]. PAA possesses highly ordered nanopores with controllable and homogeneous dimensions arranged in a close-packed hexagonal pattern. Up to date, PAA films with pore diameter ranging from 4 nm to 420 nm, density as high as 10^{15} pores/m², and film thickness varying from 0.1 μm to 300 μm have been realized using two-step anodization or via prepatterning methods [2–7]. Just recently, Miao Chen group in China has reported a facile single side and two-step anodization approach without any special pretreatment to formation of highly ordered through-hole porous anodic aluminum films [8].

In 1970, O'Sullivan and Wood [9] presented a model to describe the self-regulating pore growth based on the electric field distribution at the pore bottoms. This and further re-fined models [10–12] gave some microscopic explanations for the dependence of, the pore diameters and the pore distances on the anodizing conditions. In National Technical University of Athens, Patermarakis [13–15] has deeply researched the kinetics and mechanism of growth and the structure of PAA, based on the determination of the composition of the anodizing solution inside the pores by considering the mass and charge transport phenomena during the growth of PAA films. Shawaqfeh and Baltus [16] repoeted their studies on the growth kinetics of porous alumina films formed by anodic oxidation of aluminum in phosphoric acid under galvanostatic conditions based on the interplay between film growth and oxide dissolution that controls the resulting film morphology.

Recently, PAAs have been widely used as templates to fabricate a variety of nanomaterials such as high density storage media, optical and magnetic functional nanomaterials exhibiting quantum size effect, highly sensitive chemical sensors, nano electronic devices and functional bio-chemical membranes [17].

N.-Q. Zhao · X.-X. Jiang · C.-S. Shi · J.-J. Li ·
Z.-G. Zhao · X.-W. Du (✉)
School of Materials Science & Engineering,
Tianjin University, Tianjin 300072, China
e-mail: xwdu@tju.edu.cn

Highly regular pore structures occur only for a quite small processing window, whereas an amorphous pore structure can be obtained for a very wide range of parameters without substantial change in morphology. In this work, the dependences of structural properties and regularity of PAA and steady current density on anodizing conditions have been investigated to gain more insights into the formation conditions of highly ordered pore arrays. Alumina nanowires (ANWs) were fabricated simply by anodization at higher voltage. The relationship between steady current density and anodic alumina structure was taken into consideration.

Experiments

High purity (99.999%) aluminum foils (20×20 mm^2) with 0.2 mm thickness were used as the raw material. PAAs were prepared by typically two-step anodization. Prior to anodizing, the aluminum foils were annealed in nitrogen atmosphere at 500 °C for 4 h in order to enlarge the grain size and to obtain homogeneous microstructure for pore growth over large areas. Subsequently, the foils were chempolished in a 10 wt% NaOH solution. The pretreatments of annealing and chempolishing are essential to prepare more ordered pore domains. The pretreated Al foils were anodized to form PAA films in oxalic acid under appropriate anodizing voltages (20–60 V) at the temperature of 17 °C for 8 h. Subsequently, the surface film was chemically removed in the mixture solution of phosphoric acid (0.4 mol/L) and chromic acid (0.2 mol/L). Re-anodization was lasted for 10 h under the same conditions.

During anodizing, a digital amperemeter was connected in the current circuit to take record the current. The micrographs of PAA and ANW were characterized by JEOL JSM-6335F field emission scanning electron microscope (FESEM). The average pore diameter, interpore distance and statistical standard deviation of the pore diameter were statisticed by origin 7.0 according to the digital pictures. X-ray diffraction (XRD) of PAA and ANW were analyzed by Rigaku D/Max-2500 system.

Results and discussion

Figure 1 shows the relationship between the anodizing steady current density and the voltage in different concentration of the oxalic acid electrolytes. It presents that the steady current density is almost exponential with the voltage in the given
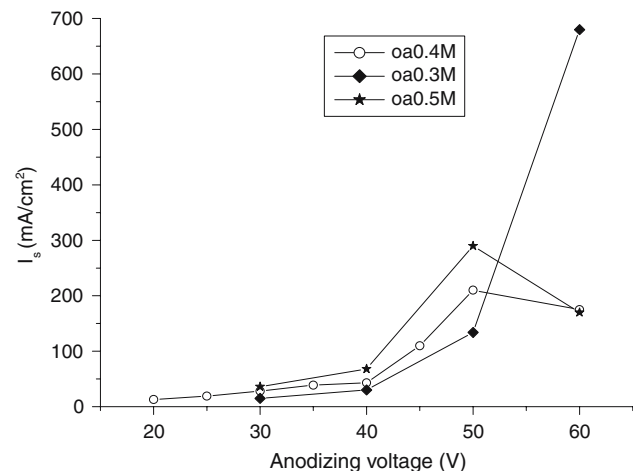

Fig. 1 The relationship between the pore diameter and the anodizing voltage and the steady current density in 0.3–0.5 M oxalic acid anodic electrolyte

electrolyte. At lower voltage, the concentration of the oxalic acid effects weakly on the steady current density, whereas it becomes more and more obviously along with the increase of the voltage. The effects of the concentration of the oxalic acid on the pore diameter and the inter-pore distance at 30 and 50 V anodizing voltage were presented in Fig. 2. It reveals clearly that the pore diameter enlarges linearly when the concentration of electrolyte increases, but the inner-pore distance does not alter under a given anodizing voltage. It should be noted that the pore diameter changes more greatly under 50 V than 30 V along with the increase of the concentration of oxalic acid. This is consistent with the obvious changes of steady current density at 50 V in Fig. 1. It demonstrates that the effect of electrolyte concentration on the pore diameter become more evident at higher voltage. At the same time, the experiment results indicate that the relationship between the pore diameter and the voltage is almost linear in a given electrolyte.

According to the model of PAA proposed by O'Sullivan and Wood [9], the thickness of barrier layer (l) is equal to a half of the thickness of inner wall approximately, and the thickness of inner wall is determined by inter-pore distance (D) minus pore diameter (d). It can be figured as the following formula.

$$l = (D - d)/2 \tag{1}$$

During the anodizing process, the resistance focuses on the barrier layer. Therefore the electric field intensity (E) between inner and outer of barrier layer
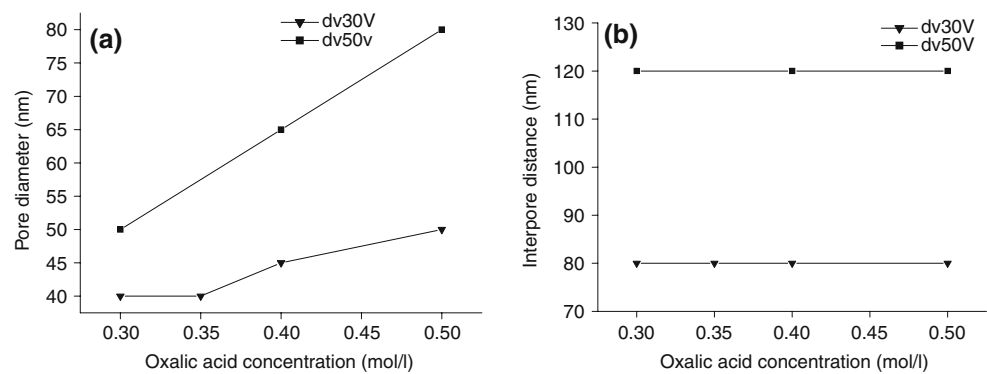
lies on the voltage and barrier layer thickness. The electric field intensity is given by

$$E = V/l \qquad (2)$$

where V is the voltage between the inner and outer of barrier layer (equals to the anodizing voltage), l the barrier layer thickness.

The current density in the circuit is determined by

$$I_s = A \exp(BE) \qquad (3)$$

where A and B are coefficient related to temperature, E the same with (2).

In a given electrolyte, both D and d enlarge along with the increase of the anodizing voltage, whereas the change of the barrier layer thickness is negligible. According to Eq. 1–3, it can deduce that the current density is exponential with the voltage.

Based on the comparison of the statistical standard deviations of the pore diameter for PAAs formed at different anodizing voltage (30–60 V) in 0.3 M oxalic acid, the relative symmetrical PAA was determined. We can found that the suited anodizing voltage for 0.3 M oxalic acid is 30 V. In the same way, the suited anodizing voltages for 0.4 and 0.5 M oxalic acid electrolytes can be confirmed. Table 1 shows the suited anodizing conditions and structure parameters for the PAAs with regular pores arrange-

ments. The SEM micrographs of PAAs with higher ordered arranged pores arrays are shown in Fig. 3. Almost perfect hexagonal ordered can be observed over a wide range of grain domains. It can be seen that at when the anodizing voltage range from 30 V to 50 V, regular pores with 40–80 nm size can be obtained.

It should be noticed that some disordered ANWs were achieved at the anodizing voltage of 60 V in 0.4 and 0.5 M oxalic acid solution, as shown in Fig. 4. Figure 5 presents the XRD spectrum of PAA (0.5 M $H_2C_2O_4$, 50 V) and ANW (0.5 M $H_2C_2O_4$, 60 V). It can be seen that the both spectrums of PAA and ANW have the same characterization. A non-spiculate diffraction peaks at $2\theta = 27.5°$ in both spectrums indicate the amorphous alumina. The other three diffraction peaks at $2\theta = 44.7, 65.0°$ and $78.1°$ are well coincident with the substructure aluminum.

Based on the former analysis, the anodizing voltage lying within only a small window, the pore diameter matches the inter-pore distance perfectly, and then regular nanopore arrangements is obtained. It has also been shown that, for a given anodizing electrolyte, the pore diameter and the inter-pore distance enlarge linearly nearly, and barrier layer thickness does not alter. There is a triple point [18] at the thicker intersection of every three neighbor pores, which is of great importance in the formation of less ordered PAAs and ANWs. At lower anodizing voltage, the disordered smaller pores maybe formed at the triple points, which are wider than pore diameter, and then results in less ordered porous alumina. This can be shown clearly in Fig. 6.

On the other hand, higher voltage may induce the collapsing of the thin inner wall during a long time anodizing. The triple points were left at the surface of aluminum alone, and then ANWs were obtained. At the same time, the fallen disordered ANWs result in a increase of the resistance and a decrease of the steady current density in the circuit. It is confirmed in Fig. 1 at

Table 1 Structural properties of porous anodic alumina (PAAs) analyzed from SEM images in Fig. 3

Sample	(COOH)$_2$ concentration (mol/l)	Voltage (V)	Pore diameter (nm)	Inter-pore distance (nm)	Inner wall thickness (nm)
A	0.3	30	40	80	40
B	0.4	40	50	100	50
C	0.5	50	80	120	40

Fig. 3 SEM micrographs of
porous anodic alumina
(PAAs) formed in different
anodizing conditions: (**a**)
0.3 M oxalic acid/30 V, (**b**)
0.4 M oxalic acid/40 V, (**c**)
0.5 M oxalic acid/50 V
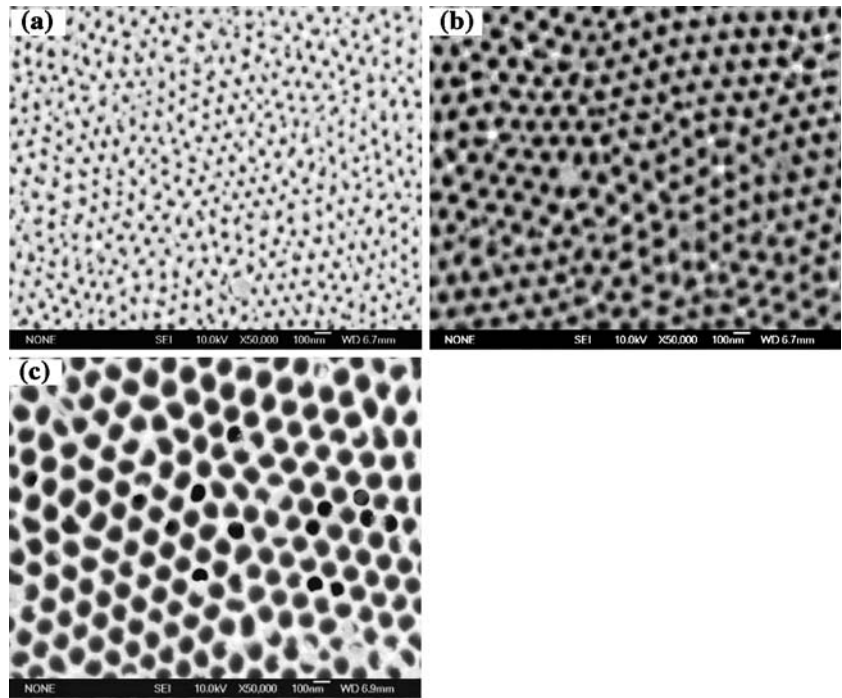
60 V anodizing voltage in 0.4 M and 0.5 M oxalic acid. The formation mechanics of the ANWs is presented in Fig. 7. But the higher anodizing voltage is not the only reason to form the ANWs [19]. Higher voltage matching with the high concentration of the electrolyte and the high temperature is the sufficiency for the formation of the ANWs. The Voltage, electrolyte concentration and reaction temperature are three main deciding elements for the structure of PAA. The increase of the three parameters can enlarge the pores and raise the ratio of the pore diameter and the interpore distance without exception. In other words, the relative thickness of inner wall is decreased, which play an important part in the formation of anodic ANWs. In addition, the increase of the three parameters causes the raising of current density sharply. Further studies should be done to explain the formation mechanics of ANWs.
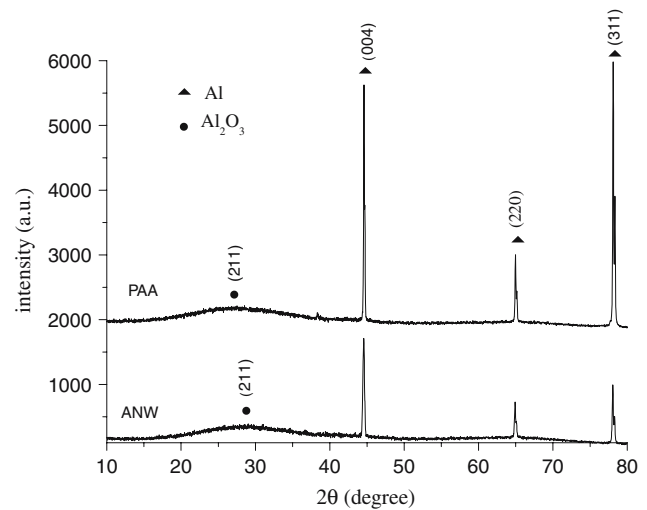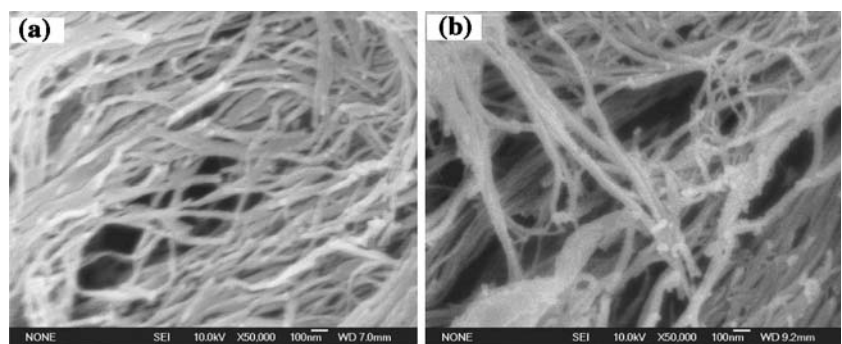

Fig. 5 XRD spectrum of the porous anodic alumina (PAA) (0.5 M oxalic acid, 50 V) and alumina nanowire (ANW) (0.5 M oxalic acid, 60 V)

Fig. 4 SEM micrographs of
alumina nanowires (ANWs)
fabricated in (**a**) 0.4 M oxalic
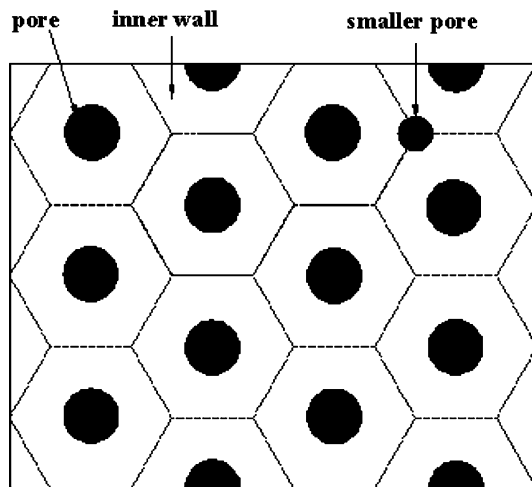acid/60 V and (**b**) 0.5 M
oxalic acid/60 V

Fig. 6 The schematic plan for the formation of disordered porous anodic alumina (PAA) at lower anodizing voltage
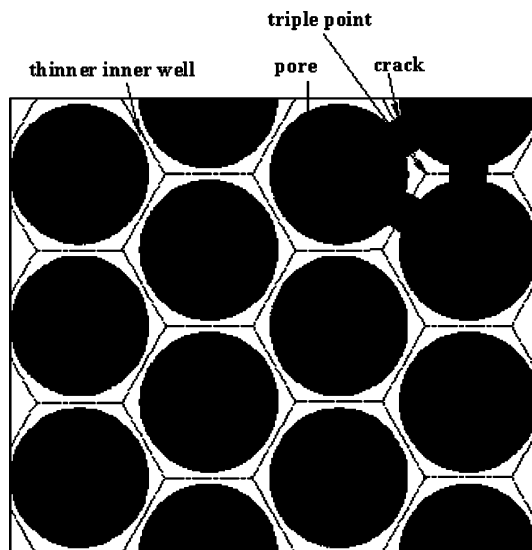

Fig. 7 The schematic plan for the formation of anodic alumina nanowires (ANWs) at higher anodizing voltage

Conclusion

In oxalic acid electrolyte, the PAA with 40–80 nm diameter were fabricated by a two-step anodization

processing. In a given electrolyte, the steady current density is dependent on the anodizing voltage exponentially. The relationship between the concentration of electrolyte and the pore diameter is almost linear, but the concentration of electrolyte has no obvious effect on the inner-pore distance. The effect of the concentration of oxalic acid on the pore diameter becomes more obvious along with the increase of the anodizing voltage. Only in a given electrolyte matching a specifically anodizing voltage, the regular nano-pore arrangements can be obtained. A higher voltage induces the collapse of thinner inner wall, and determines the achievement of disordered ANW at the triple points.

References

1. Keller F, Hunter MS, Robinson DL (1953) J Electrochem Soc 100:411
2. Masuda H, Fukuda K (1995) Science 268:1466
3. Shingubara S, Okino O, Sakaue H et al (1997) Jpn J Appl Phys 36:7791
4. Li AP, Muller F, Birner A et al (1998) J Appl Phys 84:6023
5. Li AP, Muller F, Birner A et al (1999) J Vac Sci Technol A 17:1428
6. Xu T, Zangari G, Metzger RM (2002) Nano Lett 2:37
7. Masuda H, Yamada H, Saitoh M et al (1997) Appl Phys Lett 71:2770
8. Zhao YC, Chen M, Zhang YN et al (2005) Mater Lett 59:40
9. Wood GC, O'Sullivan JP (1970) Electro Acta 15:1685
10. Thompson GE, Wood GC (1981) Nature (London) 290, 230
11. Parkhutik VP, Shershulsky VI (1992) J Phys D: Appl Phys 25:1258
12. Masuda H, Hasegwa F, Ono S (1997) J Electrochem Soc 144:L127
13. Patermarakis G, Moussoutzanis K (1995) J Electrochem Soc 142(3):737
14. Patermarakis G, Moussoutzanis K (1995) Electrochim Acta 40(6):699
15. Patermarakis G (1998) J Electroanal Chem 447:25
16. Shawaqfeh AT, Baltus RE (1998) J Electrochem Soc 145(8):2699
17. Shingubara S (2003) J Nano Res 5:17
18. Mei YF, Siu GG, Fu RKY et al (2005) J Appl Phys 97
19. Zhao YC, Chen M, Xu T et al (2005) Coll Surf (A): Physchem Eng 257–258:363